The role of albedo and accumulation in the 2010 melting record in Greenland

2011 Environ. Res. Lett. 6 014005

Environ. Res. Lett. **6** (2011) 014005 (6pp) doi:10.1088/1748-9326/6/1/014005

The role of albedo and accumulation in the 2010 melting record in Greenland

M Tedesco[1], X Fettweis[2,3], M R van den Broeke[3], R S W van de Wal[3], C J P P Smeets[3], W J van de Berg[3], M C Serreze[4] and J E Box[5,6]

[1] The City College of New York, CUNY, New York, NY, USA
[2] University of Liège, Liège, Belgium
[3] Institute for Marine and Atmospheric Research Utrecht (IMAU), Utrecht University, Utrecht, The Netherlands
[4] National Snow and Ice Data Center, Boulder, CO, USA
[5] Department of Geography, Ohio State University, Columbus, OH, USA
[6] Byrd Polar Research Center, Ohio State University, Columbus, OH, USA

Received 1 December 2010
Accepted for publication 7 January 2011
Published 21 January 2011
Online at stacks.iop.org/ERL/6/014005

Abstract
Analyses of remote sensing data, surface observations and output from a regional atmosphere model point to new records in 2010 for surface melt and albedo, runoff, the number of days when bare ice is exposed and surface mass balance of the Greenland ice sheet, especially over its west and southwest regions. Early melt onset in spring, triggered by above-normal near-surface air temperatures, contributed to accelerated snowpack metamorphism and premature bare ice exposure, rapidly reducing the surface albedo. Warm conditions persisted through summer, with the positive albedo feedback mechanism being a major contributor to large negative surface mass balance anomalies. Summer snowfall was below average. This helped to maintain low albedo through the 2010 melting season, which also lasted longer than usual.

Keywords: Greenland, melting, surface mass balance, albedo, accumulation

1. Introduction and objectives

Large positive near-surface temperature anomalies occurred along the coast of the Greenland ice sheet during the year 2010 (e.g., Box *et al* 2010). For example, at Aasiaat (68°42′35″N 52°52′10″W) along Greenland's west coast, 2010 as a whole was the warmest since records began in 1951, with records also set for winter, spring, May and June. Narsarssuaq (61°09′39″N 45°25′32″W) in southern Greenland, saw its warmest winter and spring, its warmest May, and its warmest annual average since records began in 1951; Nuuk, the capital of Greenland, located along the southwest coast (64°10′30″N, 51°44′20″W), with a temperature time series extending back to 1873, saw record warmth for winter, spring, summer and the year as a whole (Cappelen 2010).

Surface melting over the Greenland ice sheet, which can be estimated from satellite data, ground observations or models (Abdalati and Steffen 1997, Mote 2007, Nghiem *et al* 2001, Hall *et al* 2009, Tedesco 2007, Hanna *et al* 2008, Fettweis *et al* 2010b, Ettema *et al* 2010) was also exceptional in 2010 (Box *et al* 2010). Results obtained by applying the algorithm reported in Tedesco (2007) to spaceborne microwave brightness temperatures (e.g., Armstrong *et al* 1994, Knowles *et al* 2002) are consistent with those reported in Box *et al* (2010), showing that large areas of the ablation zone in south Greenland underwent melting up to 50 days longer in 2010 compared to the 1979–2009 average, with melting in 2010 starting exceptionally early at the end of April and ending quite late in mid September (figure 1). These results are confirmed by surface measurements.

Near-surface air temperature is often used as a proxy for surface melting. Previous studies have analyzed exceptional melting events mainly focusing on the relationship between melt and near-surface temperatures (e.g., Mote 2007, Tedesco

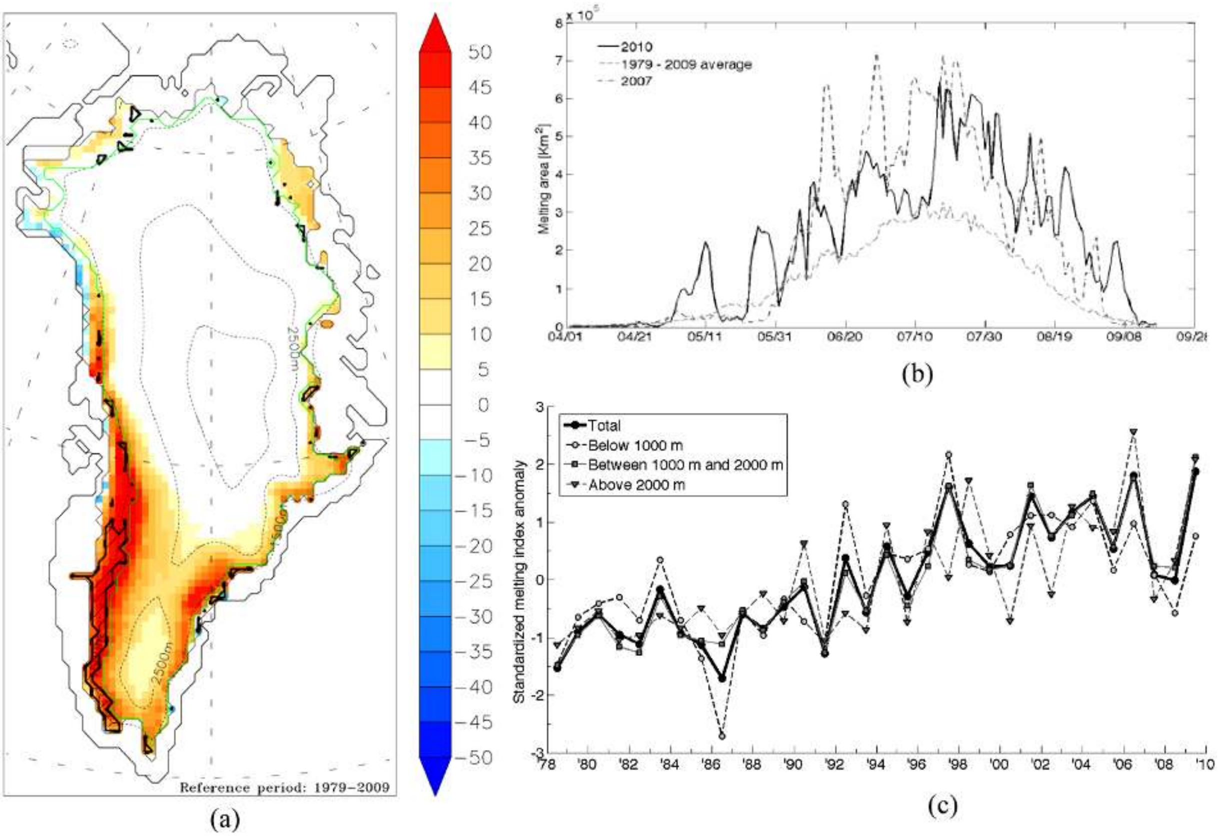

Figure 1. (a) anomaly map of melting days for 2010 derived from passive microwave data. Hatched regions indicate where MAR-simulated meltwater production exceeds the mean by at least two standard deviations; (b) time series of the daily melt extent for the 2010 season, the 1979–2009 average and the year 2007; (c) standardized melting index (the number of melting days times area subject to melting) for 2010 from passive microwave data over the whole ice sheet and for different elevation bands.

2007). However, melting and the surface mass balance (SMB), also depend on accumulation, radiation conditions, refreezing and sublimation, the latter relatively small and constant in time (Box and Steffen 2001, Fettweis 2007, van den Broeke *et al* 2008). Surface melt and albedo are intimately linked: as melting increases, so does snow grain size, leading to a decrease in surface albedo which then fosters further melt. Also, changes in accumulation can affect the seasonal evolution of surface albedo, which influences the SMB. It is hence not sufficient to analyze near-surface temperature trends to understand the driving mechanisms of extreme mass loss, and studying the role of albedo and accumulation becomes crucial to provide a more robust understanding of the exceptional melting detected by satellite microwave sensors.

In this study, we report results derived from spaceborne sensors, surface glaciological observations and regional atmospheric model outputs regarding the surface albedo, accumulation and bare ice exposure over the Greenland ice sheet during the summer of 2010. Our results indicate that negative surface albedo anomalies were especially prominent over west Greenland, with bare ice exposed earlier than previous years. In addition, increased runoff and reduced accumulation likely contributed to a strongly negative SMB.

2. Data and methodologies

2.1. Satellite data

We use the moderate-resolution imaging spectroradiometer (MODIS) 16-day gridded albedo product (http://www-modis.bu.edu/brdf/userguide/intro.html) to study anomalies in both directional hemispherical reflectance (black-sky albedo) and bi-hemispherical reflectance (white-sky albedo) in the shortwave, visible and near-infrared bands. Black-sky albedo is the albedo under direct illumination (or direct beam contribution), whereas white-sky albedo is the one under diffuse or indirect light. Black- and white-sky albedos can be combined as a function of the diffuse skylight for a representation of the actual albedo such as measured by field instruments (Lucht *et al* 2000). The MODIS product, which has been evaluated over Greenland (e.g. Stroeve *et al* 2005), is provided every 8 days using 16 days acquisitions from both the TERRA and AQUA satellites. Data are provided on a 0.05° latitude/longitude grid. While we discuss only the shortwave white-sky albedo, the conclusions that follow also apply to black-sky, visible and near-infrared albedos.

2.2. Glaciological data

The Institute of Marine and Atmospheric Research Utrecht, (IMAU) installed several automatic weather stations (AWSs)

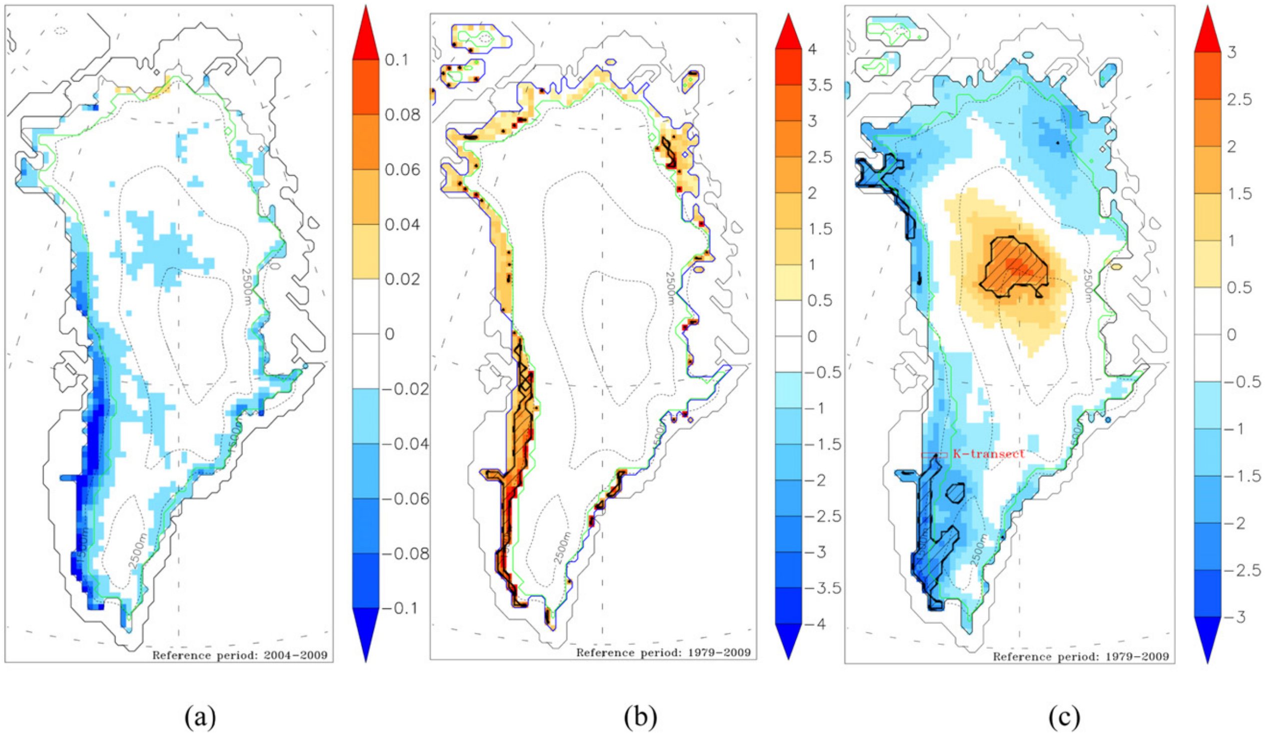

Figure 2. (a) MODIS shortwave white-sky albedo anomalies for 2010, relative to 2004–2009 means for May–August; (b) MAR estimated standardized anomalies (relative to 1979–2009) of the number of days with bare ice exposed for the period May–September; (c) May–September snowfall anomalies from MAR, relative to 1979–2009 means.

along the Kangerlussuaq transect (K-transect, 67°N) in southwest Greenland in August 2003, located at increasing distance from the ice sheet margin and increasing elevations, up to 1500 m a.s.l. (van den Broeke *et al* 2008). This part of Greenland is characterized by a 100 km wide ablation zone and an average equilibrium line altitude (ELA) of approximately 1500 m a.s.l. The stations are equipped with radiation sensors. SMB can be estimated at the local spatial scale from stakes and acoustic height rangers. Apart from atmospheric radiation, the stations measure basic meteorological variables like wind speed and direction, temperature, relative humidity and air pressure. SMB measurements are performed along the K-transect at selected sites. The three AWS sites (S5, S6 and S9) are located, respectively, 6 km (S5), 37 km (S6) and 91 km (S9) from the ice sheet margin at an elevation of 490 m (S5), 1020 m (S6) and 1520 m (S9) a.s.l. Mass balance sites (S4, SHR, S7, S8, S10) are located 3 km (S4), 14 km (SHR), 52 km (S7), 63 km (S8) and 143 km (S10) from the ice sheet margin at an elevation of 340/390 m (S4, 340 m was the initial value), 710 m (SHR), 1110 m (S7), 1260 m (S8) and 1850 m (S10) a.s.l. Mass balance data are available over the period 1991–2010. Weather station data are available for the period 2003–2010. Further information on the stations can be found in van de Wal *et al* (2005).

2.3. The surface and energy balance model

The surface and energy balance model is the regional climate model MAR (Modèle Atmosphérique Régional), coupled to the 1D Surface Vegetation Atmosphere Transfer scheme SISVAT (Soil Ice Snow Vegetation Atmosphere Transfer). The schemes and the set-up employed for the present study are fully described in Fettweis *et al* (2010a), Fettweis (2007) and Lefebre *et al* (2005). Differently from most existing models, MAR is coupled to a snow physical model called CROCUS (Brun *et al* 1992). CROCUS is a one-dimensional multi-layered energy balance model consisting of a thermodynamic module, a water balance module taking into account the refreezing of meltwater, a snow metamorphism module, a snow/ice discretization module and an integrated surface albedo module. For this study, MAR outputs are derived at a spatial resolution of 25 km for the period 1958–2010. The ERA-40 reanalysis (1957–2001), the ERA-INTERIM reanalysis (2002–June 2010) and after that, the operational analysis (July 2010–September 2010) from ECMWF are used to initialize the meteorological fields at the beginning of the simulation in September 1957 and to force every 6 h the lateral boundaries with temperature, specific humidity and wind components during the simulation. The sea surface temperatures (SST) and the sea-ice extent in the SISVAT module are also prescribed by the reanalyses. No re-initialization or correction are applied to the model outputs. The (re)analysis data are available every 6 h at a resolution of at least 1°. The MAR spatial domain is represented by an area of 2000 km × 3500 km centered at 70°N latitude and 40°W longitude. There are at least ten pixels between the Greenland and the model boundaries. The integration domain is shown in Fettweis *et al* (2005). An ice sheet mask is then applied to analyze only those pixels belonging to the ice sheet (Fettweis 2008). Outputs from the MAR model have been shown to be consistent with results obtained from passive microwave observations (Fettweis *et al* 2010b).

3. Results and discussion

Figure 2(a) shows the MODIS shortwave white-sky albedo anomaly for the months of May–August (MJJA), relative to the 2004–2009 mean. This period was chosen because ground albedo measurements for comparison are available starting in 2004. The MODIS record itself spans a longer period, 2001–2009. The strong negative albedo anomalies along the southwest margin of the ice sheet (more than −0.10) are consistent with the positive melting anomalies detected by the microwave sensors and simulated by the MAR model (see figure 1). As assessed using the complete MODIS record, the shortwave 2010 albedo averaged over MJJA was up to 0.15 below the mean over southwest Greenland, with the largest negative anomalies during August. August albedo anomalies are as large as −0.25 near the Nuuk area and −0.2 along most of the southwestern regions of the Greenland Ice Sheet. The observed 2010 albedo anomalies can be the consequence of: (1) a reduced frequency and/or amount of snowfall; (2) enhanced melting; and (3) exposure of bare ice for a longer period of time during the melting season. Figure 2(b) provides the standardized anomaly map (the departure from the mean divided by the standard deviation of the distribution) of the number of days when bare ice was exposed in 2010 based on MAR outputs. According to MAR, in 2010 bare ice was exposed for a period up to four times longer than the standard deviation computed over the 1979–2009 period along the western region of the ice sheet, with absolute anomalies peaking up to 50 days. Figure 2(c) shows the summer snowfall anomalies (in mm water equivalent, WE) from MAR, still relative to 1979–2009 means. The model suggests that summer accumulation in 2010 over the southwestern part of the Greenland ice sheet was two standard deviations below the 1979–2009 mean. This, together with large positive near-surface temperature anomalies, very likely led to the premature exposure of bare ice (figure 2(b)) and the reduced albedo (figure 2(a)).

Figure 3(a) summarizes MAR estimates and measurements on the ice of SMB (mWE) averaged over four IMAU AWSs (SHR, S6, S8 and S9). Data from the AWSs indicate that average SMB values in 2010 were 2.3 standard deviations below the 1991–2010 average (the record from the stations begin in 1991). Moreover, according to MAR, average SMB values in 2010 at the IMAU stations locations were 2.3 standard deviations below the average over the same period. For both measured and modeled quantities, the SMB in 2010 was the lowest for the data record. As an example, figure 3(b) shows the time series of MODIS and IMAU surface albedos for 2010 together with the 2004–2009 average values at the S9 station (67°03′02″N, 48°13′53″W, 1500 m a.s.l.). Differences in absolute values from the satellite and ground observations reflect the spatial scale at which MODIS data are collected or re-gridded, atmospheric corrections, and the MODIS albedo retrieval algorithm. The figure highlights that both MODIS and the station data show a decline in albedo through the 2010 melting season, with the absence of sporadic peaks that would result from snowfall events (which are present during years when positive anomalies of summer snowfall are measured and modeled). The match between the seasonal trends derived from MODIS and those measured on the ice lends credence to the MAR results, pointing to negative snowfall anomalies for 2010 (figure 2(c)) and premature exposure of bare ice (figure 2(b)).

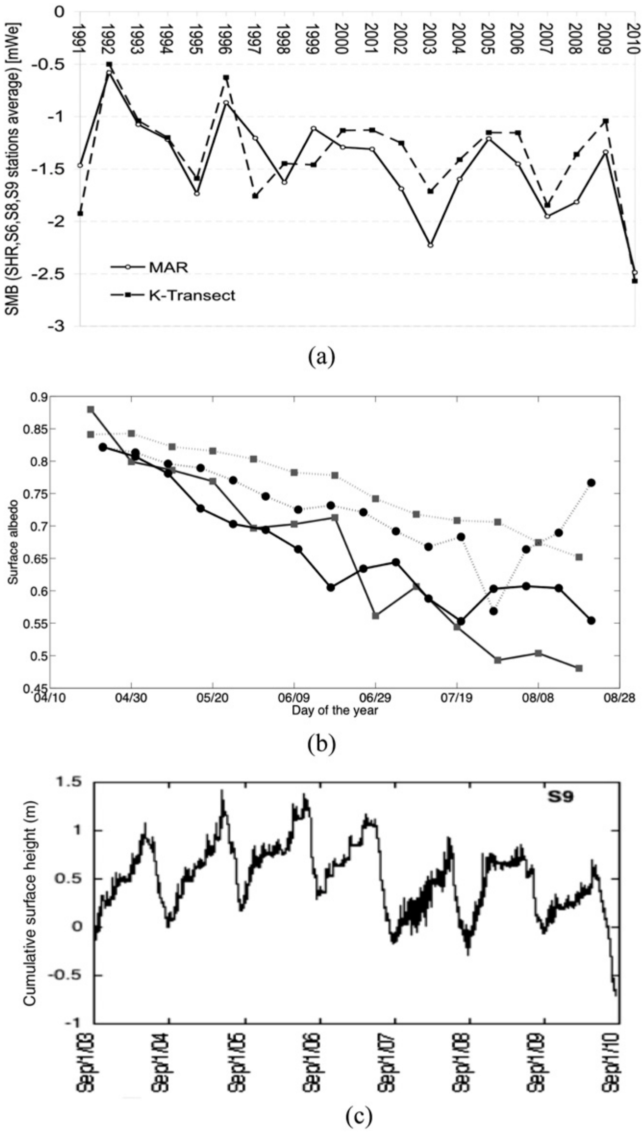

Figure 3. (a) SMB from MAR and from sonic height ranger data (K-transect) for 1991–2009 averaged over the S9, S8, S6 and SHR stations; (b) time series of MODIS shortwave albedo (black lines with circles) and albedo at the IMAU sites (gray lines with squares) for 2010 at the S9 station. Dotted lines indicate averages for 2004–2009; (c) data from the sonic height ranger collected every half an hour over the last 7 years (September 2003–September 2010) at the S9 station.

Early exposure of bare ice and reduced snowfall in 2010 are also evident from surface height measurements along the K-transect. Figure 3(c) illustrates surface height changes over the years 2003–2010 at the S9 station. We focus on the station S9 as it is situated at 1500 m elevation, at the approximate

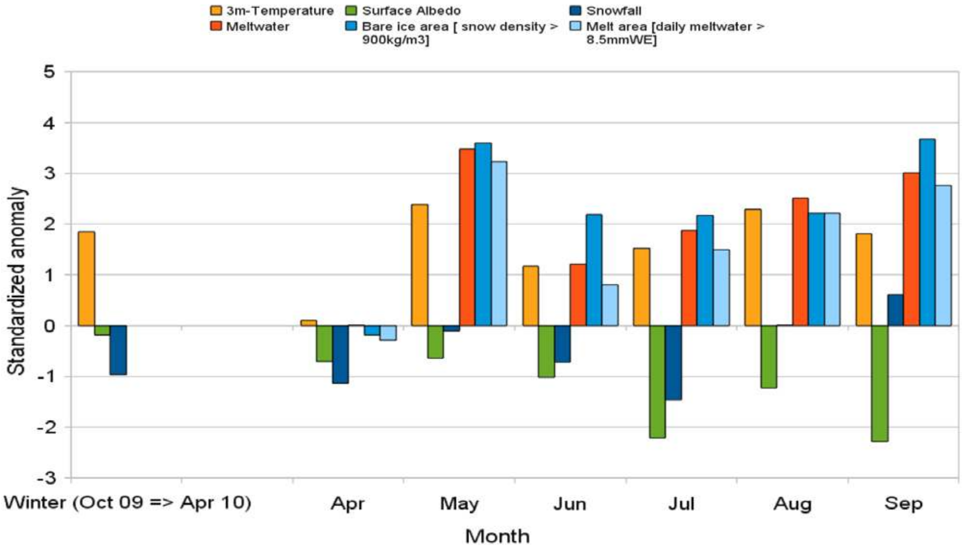

Figure 4. Monthly standardized anomalies for 2010 (relative to 1979–2009) for near-surface temperature, albedo, snowfall, meltwater, bare ice area and melt area excluding bare ice simulated by MAR.

ELA, where annual accumulation should on average equal ablation. From figure 3(c), the net annual surface height change for the years 2004, 2007 and 2008 is close to 0 m (indicating that the position of the ELA was close to the station elevation), contrasting with the years of 2005 and 2006 when the net surface height change was ∼0.3–0.4 m (indicating that the station was above the ELA for those years). Reduced accumulation and exceptionally large ablation during 2010 are evident. The surface height data clearly indicate that accumulation for 2010 at the S9 station was only about 0.6 m (versus the 2003–2009 average of ∼1.05 m) and the surface height value recorded at the end of August was −0.7 m (versus the 2003–2009 average of ∼−0.05 m), below any value previously recorded. The total change in surface height was ∼1.3 m, the highest loss over the past twenty years. The extreme nature of the SMB loss in 2010 is also evident at the other stations along the K-transect (not shown here).

The MAR allows us to examine conditions back to 1958, placing 2010 in the context of a longer time series. According to MAR, the hydrological year (October–September) 2009–2010 SMB anomaly set a new record low of −310 Gt, 2.6 standard deviations below the 1958–2009 average, surpassing the previous record of 2.3 standard deviations set in 2007. Snowfall for the period 1 October 2009–30 September 2010 was about 68 Gt (1.5 standard deviations below average) and runoff was 243 Gt, or 2.4 standard deviations above the 1958–2009 average. Figure 4 shows monthly standardized anomalies for 2010 (using 1979–2009 as a reference for consistency with the passive microwave data time series) from MAR of near-surface temperature, albedo, snowfall, meltwater, bare ice area and melt area excluding bare ice. Snowfall and near-surface temperature anomalies for the autumn and winter of 2009 (September–April) are also reported as a reference. The model indicates that surface albedo was persistently below the average (two standard deviations) for the summer. The meltwater produced in May (August) was ∼3 (∼2.5) standard deviations above the mean. Bare ice area in May was ∼3.5 standard deviations above the mean and it remained persistently around two standard deviations above average through summer. By contrast, the melt area excluding bare ice was exceptional in May, August and September.

4. Conclusions

Our analysis of remote sensing data, surface glaciological observations and model outputs paints a portrait of strongly negative surface mass balance during 2010 promoted by a strong warmth and enhanced by large negative anomalies of albedo and accumulation and large positive anomalies of days when bare ice was exposed. Our results clearly indicate that, beside near-surface temperature, other factors must be considered to properly analyze extreme events such as the one that occurred in 2010. The melt season started in mid April, after a warm and dry winter. Early melt onset, triggered by large positive near-surface temperature anomalies during May 2010 (up to +4 °C above the mean) contributed to accelerated snowpack metamorphism and premature bare ice exposure, with the consequence of rapidly reducing the surface albedo. Reduced accumulation in 2010, and the positive albedo feedback mechanism are likely responsible for the premature exposure of bare ice. While June and July temperature anomalies were not exceptional, being +1.5 °C above the 1979–2009 average, anomalously warm conditions persisted with the positive albedo feedback mechanism contributing to large negative SMB anomalies. Summer snowfall, which helps to increase surface albedo, was below average. Melt during August and September was also exceptional, consistent with low surface albedos and near-surface temperature anomalies of up to +3 °C, yielding a long ablation season.

The surface melt time series from the combined passive microwave record, 1979–present, is characterized by an upward trend, with considerable year-to-year variability primarily related to atmospheric conditions. Viewed in this context, the unusually warm conditions over the Greenland ice sheet in 2010 and reduced snowfall can be related to persistence of a 500 hPa high ridge from late spring through summer. Averaged for May–August, 500 hPa heights were above normal over all of Greenland, with the largest anomalies of up to 80 m over the south-central ice sheet. This anomalous ridge was associated with 700 hPa temperature anomalies over south-central Greenland of up to +3 °C. The ridge and associated 700 hPa temperature anomaly was best expressed in May and August, coinciding with near-surface air temperature records.

Acknowledgments

This work was supported by NSF grants ANS 0909388 and ARC 0901962, the NASA Cryosphere Program, and the Ohio State University Climate Water and Carbon Program. Field work along the K-transect has been supported by NWO/ALW.

References

Abdalati W and Steffen K 1997 Snowmelt on the greenland ice sheet as derived from passive microwave satellite data *J. Climate* **10** 165–75

Armstrong R L, Knowles K W, Brodzik M J and Hardman M A 1994 *DMSP SSM/I Pathfinder Daily EASE-Grid Brightness Temperatures* (Boulder, CO: National Snow and Ice Data Center, Digital Media) updated 2009

Box J E, Cappelen J, Decker D, Fettweis X, Mote T, Tedesco M and van de Wal R S W 2010 Greenland (in Arctic Report Card 2010, available at www.arctic.noaa.gov/reportcard)

Box J E and Steffen K 2001 Sublimation estimates for the Greenland ice sheet using automated weather station observations *J. Geophys. Res.* **106** 33965–82

Brun E, David P, Sudul M and Brunot G 1992 A numerical model to simulate snowcover stratigraphy for operational Avalanche forecasting *J. Glaciol.* **38** 13–22

Cappelen J 2010 DMI monthly climate data collection 1768–2009, Denmark, The Faroe Islands and Greenland *Dansk Meterologisk Institut* Technical Report No. 10-05 (available at www.dmi.dk/dmi/tr10-05.pdf)

Ettema J, van den Broeke M R, van Meijgaard E, van de Berg W J, Box J E and Steffen K 2010 Climate of the Greenland ice sheet using a high-resolution climate model—part 1: evaluation *Cryosph. Discuss.* **4** 561–602

Fettweis X 2007 Reconstruction of the 1979–2006 Greenland ice sheet surface mass balance using the regional climate model MAR *The Cryosphere* **1** 21–40

Fettweis X 2008 Impact of ice sheet mask and resolution on estimating the surface mass balance of the Greenland ice sheet *Proc. European Geophysical Union General Assembly (Vienna, April, 2008)* (available at http://orbi.ulg.ac.be/bitstream/2268/36752/1/Fettweis-2008-EGU-Poster2.pdf)

Fettweis X, Gallee H, Lefebre L and van Ypersele J P 2005 Greenland surface mass balance simulated by a regional climate model and comparison with satellite derived data in 1990–1991 *Clim. Dyn.* **24** 623–40

Fettweis X, Mabille G, Erpicum M, Nicolay S and van den Broeke M 2010a The 1958–2009 Greenland ice sheet surface melt and the mid-tropospheric atmospheric circulation *Clim. Dyn.* **36** 139–59

Fettweis X, Tedesco M, van den Broeke M and Ettema J 2010b Melting trends over the Greenland ice sheet (1958–2009) from spaceborne microwave data and regional climate models *Cryosph. Discuss.* **4** 2433–73

Hall D K, Nghiem S V, Schaaf C B, DiGirolamo N E and Neumann G 2009 Evaluation of surface and near-surface melt characteristics on the Greenland ice sheet using MODIS and QuikSCAT data *J. Geophys. Res.* **114** F04006

Hanna E, Huybrechts P, Steffen K, Cappelen J, Huff R, Shuman C, Irvine-Fynn T, Wise S and Griffiths M 2008 Increased runoff from melt from the Greenland ice sheet: a response to global warming *J. Climate* **21** 331–41

Knowles K W, Ein G, Njoku E, Armstrong R L and Brodzik M J 2002 *Nimbus-7 SMMR Pathfinder Daily EASE-Grid Brightness Temperatures* (Boulder, CO: National Snow and Ice Data Center, Digital Media)

Lefebre F, Fettweis X, Gallée H, van Ypersele J, Marbaix P, Greuell W and Calanca P 2005 Evaluation of a high-resolution regional climate simulation over Greenland *Clim. Dyn.* **25** 99–116

Lucht W, Schaaf C B and Strahler A H 2000 An algorithm for the retrieval of albedo from space using semiempirical BRDF models *IEEE Trans. Geosci. Remote Sens.* **38** 977–98

Mote T L 2007 Greenland surface melt trends 1973–2007: evidence of a large increase in 2007 *Geophys. Res. Lett.* **34** L22507

Nghiem S V, Steffen K, Kwok R and Tsai W Y 2001 Detection of snowmelt regions on the Greenland ice sheet using diurnal backscatter change *J. Glaciol.* **47** 539–47

Stroeve J C, Box J, Gao F, Liang S, Nolin A and Schaaf C 2005 Accuracy assessment of the MODIS 16-albedo product for snow: comparison with Greenland *in situ* measurements *Remote Sens. Environ.* **94** 46–60

Tedesco M 2007 Snowmelt detection over the Greenland ice sheet from SSM/I brightness temperature daily variations *Geophys. Res. Lett.* **34** L02504

van de Wal R S W, Greuell W, van den Broeke M, Reijmer C H and Oerlemans J 2005 Surface mass-balance observations and automatic weather station data along a transect near Kangerlussuaq, West Greenland *Ann. Glaciol.* **42** 311–6

van den Broeke M R, Smeet C J P P, Ettema J, van der Veen C, van de Wal R S W and Oerlemans J 2008 Partitioning of energy and meltwater fluxes in the ablation zone of the west Greenland ice sheet *The Cryosphere* **2** 179–89